for some $\epsilon > 0$. Let $\kappa \in \mathbf{R}^n$ be defined as $\kappa_i = k$ for all $i \in \{1, \cdots, n\}$. Define the following change of variables:

$$w(t) = \tilde{x}(t) + \kappa. \tag{19}$$

Then w satisfies

$$\dot{w} = F(t, w_t - \kappa) = G(t, w_t) = G(w_t). \tag{20}$$

We show that the FDE in (20) satisfies assumptions $H-1$, $H-2$, $H-3$, and $H-5$ in [15]. It is easy to verify that $G(2\kappa) \leq \theta$ and $G(\theta) \geq \theta$. Therefore, assumption $H-3$ is satisfied. Assumption $H-1$ is satisfied because G is globally Lipschitzian [15, remark 4]. $H-2$ is satisfied because $\tilde{A}$ has nonnegative off-diagonal elements and $\tilde{A}^\tau$ has nonnegative elements. To show that $H-5$ is satisfied, let $\xi, \eta \in \mathbf{R}^n_\mp$ be such that $\xi \leq \eta$ and $\xi \neq \eta$. Let i be an index such that $\hat{f}(\eta_i - \kappa) - \hat{f}(\xi_i - \kappa)$ has the largest value. It is clear that we can choose i such that $\eta_i - \xi_i > 0$. Then

$$\begin{aligned} G_i(\xi) - G_i(\eta) &= \eta_i - \xi_i + \sum_{j=1}^{n} (\tilde{A} + \tilde{A}^\tau)_{ij} (\hat{f}(\xi_j - \kappa) - \hat{f}(\eta_j - \kappa)) \\ &\geq \eta_i - \xi_i + (\hat{f}(\eta_i - \kappa) - \hat{f}(\xi_i - \kappa)) \sum_{j=1}^{n} -(\tilde{A} + \tilde{A}^\tau)_{ij} \\ &\geq \eta_i - \xi_i > 0. \end{aligned} \tag{21}$$

Where we have used the assumption that $\sum_{j=1}^{n} -(\tilde{A} + \tilde{A}^\tau)_{ij} \geq 0$ for all i. Therefore, $H-5$ is satisfied.

By [15, lemma 3], for all initial conditions in $C_{\tilde{\tau}}^{[\theta, 2\kappa]}$ the trajectory of (20) will converge to one equilibrium point. This means that for all initial conditions in $C_{\tilde{\tau}}^{[-\kappa, \kappa]}$ all trajectory of (2) will converge to an unique equilibrium point. By definition of k, all trajectories will eventually enter $[-\kappa, \kappa]$. Therefore, for any trajectory $\tilde{x}(t)$, there exists $T > 0$ such that $\tilde{x}_T(\cdot) \in C_{\tilde{\tau}}^{[-\kappa, \kappa]}$ and the unique equilibrium point is globally asymptotically stable. ■

The property of having a globally asymptotically stable equilibrium point allows such a CNN to be used as a pattern classifier or encoder [11] in the sense that there is a nonlinear map that relates the steady-state output to the input independent of the initial conditions. One could also view these CNN's as solving nonlinear equations in the sense that given any initial condition, the CNN will converge to the unique solution of a set of nonlinear algebraic equations with the set of equations being solved depending on the input.

IV. Conclusions

Simple and useful stability conditions have been presented in this paper for the case when the templates are dominant nonlinear and delay-type.

References

[1] L. O. Chua and L. Yang, "Cellular neural networks: Theory," *IEEE Trans. Circuits Syst.*, vol. 35, pp. 1257–1272, 1988.

[2] L. O. Chua and L. Yang, "Cellular neural networks: Applications," *IEEE Trans. Circuits Syst.*, vol. 35, pp. 1273–1290, 1988.

[3] *Proc. 1990 IEEE Int. Workshop on Cellular Neural Networks and Their Applications* 1990.

[4] T. Roska and L. O. Chua, "Cellular neural networks with nonlinear and delay-type template elements," in *Proc. IEEE Int. Workshop on Cellular Neural Networks and Their Applications*, pp. 12–25, 1990.

[5] W. Heiligenberg and T. Roska, "On biological sensory information processing principles relevant to dual computing CNN's," *Rep. DNS-4-1992*, Dual and Neural Comp. Sys. Res. Lab., Comp. Aut. Inst., Hung. Acad. of Sci., Budapest, Mar. 1992.

[6] L. O. Chua and T. Roska, "Stability of a class of nonreciprocal cellular neural networks," *IEEE Trans. Circuits Syst.*, vol. 37, pp. 1520–1527, 1990.

[7] L. O. Chua and C. W. Wu, "On the universe of stable cellular neural networks," *Int. J. Circuit Theory and Applications*, vol. 20, 1992.

[8] T. Roska, C. W. Wu, M. Balsi, and L. O. Chua, "Stability and dynamics of delay-type general and cellular neural networks," *IEEE Trans. Circuits Syst.-I*, vol. 39, pp. 487–490, June 1992.

[9] ——, "Stability and dynamics of delay-type and nonlinear cellular neural networks," *ERL Memorandum UCB/ERL M91/110*, Univ. California, Berkeley, 1991.

[10] P. P. Civalleri, M. Gilli, and L. Pandolfi, "On stability of cellular neural networks with delay," *Tech. Rep.*, Politecnico di Torino, 1992.

[11] D. G. Kelly, "Stability in contractive nonlinear neural networks," *IEEE Trans. Biomedical Eng.*, vol. 37, pp. 231–242, Mar. 1990.

[12] J. K. Hale, *Theory of Functional Differential Equations*, vol. 3 of *Applied Mathematical Sciences*. New York: Springer-Verlag, 1977.

[13] T. Roska, "Some qualitative aspects of neural computing circuits," in *Proc. IEEE Int. Symp. Circuits Syst.*, pp. 751–754, 1988.

[14] T. Roska, J. Hámori, E. Lábos, K. Lotz, L. Orzó, J. Takács, P. Venetianer, Z. Vidnyánszky, and A. Zarándy, "The CNN model in the visual pathway—part II: The amacrine cell in the modified retina model, simple LGN effects, and motion related illusions," *Tech. Rep. DNS-9-1992*, Comp. Aut. Inst. Hung. Acad. Sci., Budapest, 1992.

[15] Y. Ohta, "Qualitative analysis of nonlinear quasi-monotone dynamical systems described by functional-differential equations," *IEEE Trans. Circuits Syst.*, vol. CAS-28, pp. 138–144, Feb. 1981.

Biquadratic Transconductance Switched-Capacitor Filters

Mehmet Ali Tan

***Abstract*— Switched-capacitor (SC) filters yield efficient implementations in integrated form. However, they employ op-amps, each of which must be designed for a given filter separately. Furthermore, SC filters are not tunable. This work presents a new type of sampled data filters consisting of transconductance elements, switches and capacitors, called transconductor switched capacitor (TSC) filters. Transconductance elements do not degrade their performance within a wide frequency range and tunable ones are available.**

I. Introduction

In many real-time signal processing applications, analog sampled data filters are suitable because of the speed and the silicon area saved from analog-to-digital and digital-to-analog conversion hardware. The improvements in switched-capacitor (SC) filters have almost reached a saturation [1]. SC filters are not tunable. Accordingly, the precision of the coefficients can be increased only by increasing the area consumed by the capacitors. Furthermore, the finite op-amp gain-bandwidth degrades the performance of SC filters at relatively high frequencies [2]. The op-amps in SC filters must be compensated for stability purposes since they are always used in continuous feedback

Manuscript received December 2, 1991; revised November 17, 1992. This paper was recommended by Associate Editor D. J. Allstot.

The author is with the Department of Electrical & Electronics Engineering, Bilkent University, Bilkent 06533, Ankara, Turkey.

IEEE Log Number 9208190.

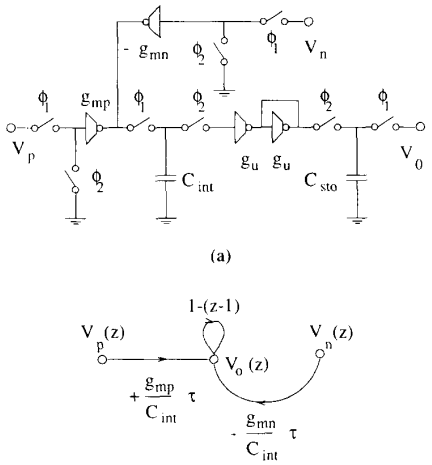

Fig. 1. (a) TSC integrator circuit and (b) its signal flow graph.

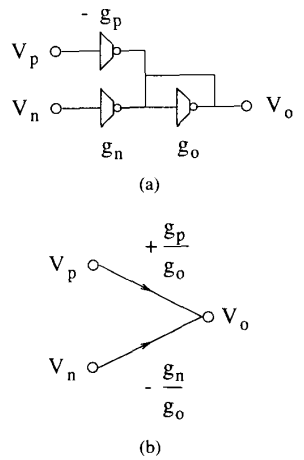

Fig. 2. (a) TSC summing circuit and (b) its signal flow graph.

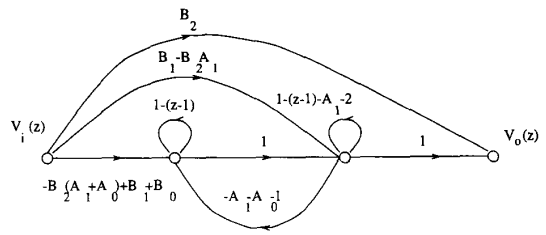

Fig. 3. A signal flow graph realizing $H(z)$ given in (3).

and must be optimized individually for given loading capacitance in order to save silicon real-estate.

This discussion suggests that transconductance elements are more suitable as active building blocks in CMOS technology. As a matter of fact, the op-amp implemented in CMOS technology behaves as a differential transconductor amplifier. Tunable and versatile transconductance elements are readily available [3]. However, Transconductance-C [4] or OTA-C [5] filters require small transconductance parameters or large capacitances which are almost infeasible for monolithic realizations in medium and low frequency range such as from the voice band to several hundred kilohertz. The switched-current filters [6] need accurate current mirror circuits because the filter coefficients are set by the current mirror ratios.

In order to some of the difficulties posed by other filter classes and capture the advantages they possess, this work introduces the transconductance switched-capacitor (TSC) filters. The TSC filters have the opportunity of using the tunable transconductances available. Furthermore, in comparison with the op-amps in SC filters, they do not need any compensation because continuous capacitive feedback does not exist in TSC filters. The filter coefficients of a TSC filter are set by the transconductance parameters, capacitor values, the clock period, and the clock pulse width.

The synthesis of TSC filters is presented based on the signal flow graph approach. The basic TSC circuits are introduced in Section II. The synthesis of TSC circuits is explained in Section III. A bandpass filter example is presented in Section IV.

II. Basic Building Blocks

The basic building blocks for the TSC ladder filters are summing discrete integrator and voltage summing circuit. All the basic circuits contain transconductance elements. A transconductance element can be modeled by a voltage controlled current source with the parameter g_m. g_m may be negative and can be obtained from the transconductance with positive g_m by a voltage inverter its input. The switches are controlled by a nonoverlapping two-phase clock with a period T. The pulse width for the phase ϕ_1 is τ. This waveform can be generated easily by a monostable circuit. The pulse width τ can be tuned by varying the time constant of the monostable circuit. The input and output signals are assumed to be sampled at the end of ϕ_1.

Integrator Circuit

In the transconductor SC integrator circuit shown in Fig. 1(a), the integrator capacitor is charged by the output currents of the transconductors g_{mn} and g_{mp} in a rate which is proportional to the piecewise-constant input signals V_n and V_p during ϕ_1. By solving the simple first order differential equation valid during ϕ_1 for the initial condition remained from the previous period, and taking the z-transform of the difference equation obtained, the input–output relationship of the integrator in the z-domain can be easily derived as

$$V_o(z) = \left[\frac{g_{mp}}{C_{int}}V_p(z) - \frac{g_{mn}}{C_{int}}V_n(z)\right]\tau\frac{1}{z-1}. \tag{1}$$

The g_u transconductances and the capacitor C_{sto} are, respectively, used to form a voltage buffer and hold the final value of the capacitor C_{int} at the output on the next ϕ_1 phase. Hence, their values do not have any significant effect on the transfer function and therefore are not important. The only requirement upon them is that the voltage of C_{sto} should be able to rise during ϕ_2. Accordingly, $C_{sto}/g_u \ll T-\tau$ condition must be satisfied. A small capacitance value may be sufficient for this purpose. A signal flow graph of the integrator circuit can be easily derived from (1) as shown in Fig. 1(b).

Summing Circuit

It can be easily shown that the transconductance circuit shown in Fig. 2(a) realizes the signed summation of two inputs as

$$V_o(z) = \frac{g_p}{g_o}V_p - \frac{g_n}{g_o}V_n \tag{2}$$

by simply writing a node equation for the output node and using the definition of transconductance elements.

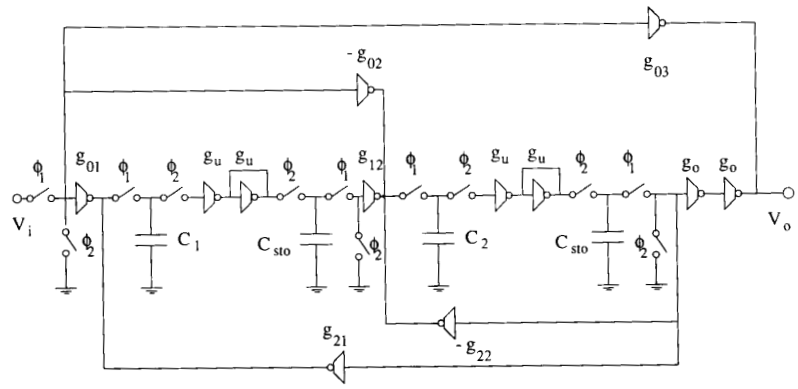

Fig. 4. Biquadratic TSC filter.

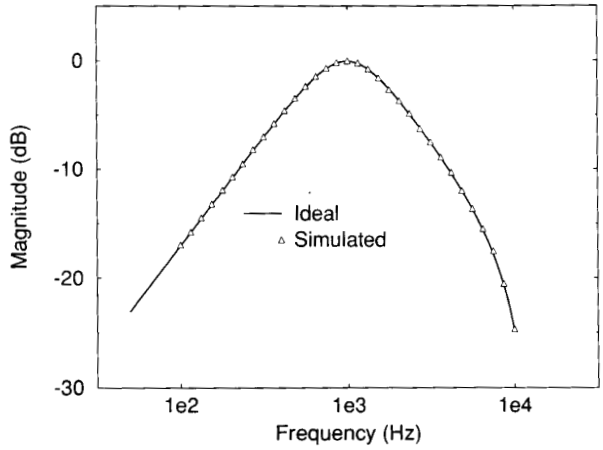

Fig. 5. Simulated and ideal magnitude characteristics of TSC bandpass filter.

A signal flow graph of this summing circuit can be easily obtained from (2) as shown in Fig. 2(b).

III. Synthesis

Although this synthesis is explained here on the biquadratic filters, it can be easily generalized and applied to the nth order filters. Let us consider the general biquadratic z-domain transfer function given as

$$H(z) = \frac{B_2 z^2 + B_1 z + B_0}{z^2 + A_1 z + A_0}. \tag{3}$$

By using well-known Mason's gain formula, it can be easily verified that the signal flow graph presented in Fig. 3 realizes $H(z)$ in (3). Note that the signal flow graph of Fig. 3 is composed of two types of subgraphs, one of which is integrator signal flow graph given in Fig. 1 and the other of which is the signal flow graph of the summing circuit given in Fig. 2. By appropriately interconnecting the subcircuits corresponding to the signal flow graph branches by appropriate element values based on the basic TSC circuits shown in Fig. 1 and Fig. 2, the resulting transconductor switched capacitor circuit is obtained as shown in Fig. 4.

IV. Example

As an example, a second-order bandpass TSC filter with a center frequency of $f_o = 1$ kHz, a quality factor of $Q = 2$, a sampling frequency of $f_c = 25$ kHz, and a duty cycle of $\tau/T = 5\%$, and the gain at the center frequency is equal to unity. A z-domain transfer function that realizes the specifications given above is

$$H(z) = \frac{0.1489(z^2 - 1)}{z^2 - 1.6427z + 0.7022}. \tag{4}$$

A set of transconductances and capacitances that realize this transfer function are chosen as

$$\begin{array}{lll} g_{01} = 1.18\mu S & g_{02} = 12.3\mu S & g_{03} = 7.4\mu S \\ g_{21} = 7.94\mu S & g_{22} = 17.5\mu S & g_{23} = 50\mu S \\ g_{12} = 50\mu S & C_1 = 30pF & C_2 = 10pF. \end{array}$$

g_u is chosen as $27\mu S$ and C_{sto}'s are chosen as 100fF.

Assuming that the transconductances with negative g_m's may consume larger chip area than the positive ones, the number of negative transmittances is reduced by scaling the appropriate branch transmittances contained in an appropriate cutset by -1. For this example the branch transmittances corresponding to g_{01}, g_{21}, and g_{12} are scaled by -1.

The time-domain simulation of the circuit using ideal switches and transconductors has been done by SPICE3d, by applying input excitations at various frequencies. The magnitude characteristic has been extracted from the simulation results and shown in Fig. 5 together with the ideal magnitude characteristic of the z-domain transfer function. The tuning can be achieved by using on of the methods which have previously suggested [7] and [8].

V. Conclusion

A new class of sampled data filters, called TSC's filters, has been presented. The synthesis of TSC filters is explained based on a signal flow graph realizing the general z-domain biquadratic transfer function. TSC filters employ transconductance elements as active devices that are readily available in various technologies and easily implemented and more suitable than op-amps in a CMOS technology. Because the building blocks are not involved in any continuous feedback any frequency compensation is not necessary for the stability purposes. The filter coefficients are determined by the clock pulse width and the transconductances, both of which can be tuned, and the integrator capacitors. This method can be easily generalized to the higher order filters.

REFERENCES

[1] R. Schaumann, K. R. Laker, and M. S. Ghausi, *Design of Analog Filters: Passive, Active RC and Switched-Capacitor.* Englewood Cliffs, NJ: Prentice-Hall, 1990.

[2] K. Martin and A. S. Sedra, "Effects of the op-amp finite gain and bandwidth on the performance of switched-capacitor filters," *IEEE Trans. Circuits Syst.*, vol. CAS-28, pp. 822–829, August 1981.

[3] C. S. Park and R. Schaumann, "A high-frequency CMOS linear transconductance element," *IEEE Trans. Circuits Syst.*, vol. CAS-33, pp. 1132–1138, 1986.

[4] R. Schaumann and M. A. Tan, "Continuous-time filter," in C. Toumazou, F. J. Lidgey, and D. G. Haigh, eds., *Analogue IC Design: The Current-Mode Approach*, ch. 9, pp. 371–386. London: Peter Perenigus, 1990.

[5] E. Sánchez-Sinencio, R. L. Geiger, and H. Nevarez-Lozano, "Generation of continuous-time two integrator loop OTA filter structures," *IEEE Trans. Circuits Syst.*, vol. 35, pp. 936–946, Aug. 1988.

[6] J. B. Hughes, "Switched-current filters," in C. Toumazou, F. J. Lidgey, and D. G. Haigh, eds., *Analogue IC Design: The Current-Mode Approach*, ch. 11, pp. 415–450. London: IEE, 1990.

[7] H. Khorramabadi and P. R. Gray, "High-frequency CMOS continuous-time filters," *IEEE J. Solid-State Circuits*, vol. SC-19, pp. 939–948, Dec. 1984.

[8] C. S. Park and R. Schaumann, "Design of a 4 MHz analog integrated CMOS Transconductance-C bandpass filter," *IEEE J. Solid-State Circuits*, vol. SC-23, pp. 987–996, Aug. 1988.

Feedback Analysis of Transimpedance Operational Amplifier Circuits

Erik Bruun

***Abstract*—The transimpedance or current feedback operational amplifier (CFB op-amp) is reviewed and compared to a conventional voltage mode op-amp using an analysis emphasizing the basic feedback characteristics of the circuit. With this approach the paradox of the constant bandwidth obtained from CFB op-amps is explained. It is demonstrated in a simple manner that the constant gain-bandwidth product of the conventional op-amp and the constant bandwidth of the CFB op-amp are both in accordance with basic feedback theory and that the differences between the traditional op-amp and the CFB op-amp are due to different ways of controlling the closed-loop gain. For the traditional op-amp the closed-loop gain is altered by altering the loop gain whereas the closed-loop gain in a CFB op-amp configuration is altered by altering the input attenuation to the feedback loop while maintaining a constant-loop gain.**

I. INTRODUCTION

The transimpedance or current feedback operational amplifier (CFB op-amp) as introduced by Nelson and Evans [1] has been available as a monolithic op-amp for a number of years. One of the most prominent features of this amplifier is the constant bandwidth, independent of the closed-loop voltage gain in a feedback configuration. This characteristic has been treated in the literature as a property almost violating traditional feedback theory that prescribes that an amplifier with feedback has a constant product of closed-loop gain and bandwidth [2], [3]. Hence, an analysis of the CFB amplifier with reference to familiar concepts in feedback theory seems appropriate.

Manuscript received September 3, 1992; revised January 6, 1993. This paper was recommended by Associate Editor B. S. Song.

E. Bruun is with the Electronics Institute, Building 349, Technical University of Denmark, DK-2800 Lyngby, Denmark.

IEEE Log Number 9208194.

II. THE VOLTAGE MODE OPERATIONAL AMPLIFIER

Fig. 1 shows a traditional voltage mode op-amp in both an inverting and a noninverting feedback configuration. Assuming that the op-amp differential voltage gain is $A_d(s)$ we find the signal flow graphs shown in Fig. 2. From these we find the closed loop $A(s)$ and the loop gain $T(s)$:

$$A(s) = \frac{\alpha A_d(s)}{1 + T(s)} \tag{1}$$

$$T(s) = -\beta A_d(s). \tag{2}$$

For the inverting amplifier we note that

$$\alpha = \frac{-R_2}{R_1 + R_2} \tag{3}$$

$$\beta = \frac{-R_1}{R_1 + R_2}. \tag{4}$$

For the noninverting amplifier we find

$$\alpha = 1 \tag{5}$$

$$\beta = \frac{-R_1}{R_1 + R_2}. \tag{6}$$

Assuming that $A_d(s) = A_0/(1 + s/\omega_c)$ we find the closed-loop gain and bandwidth relations

$$2\pi BW = \omega_c(1 - \beta A_0) \tag{7}$$

and

$$2\pi GBW = \alpha\omega_c A_0. \tag{8}$$

For the noninverting amplifier of Fig. 1(b) with $\alpha = 1$ the latter expression shows that the product of gain G and bandwidth BW is constant and equal to the unity gain bandwidth $A_0\omega_c/2\pi$ for the op-amp. For the inverting amplifier (8) shows that the product of gain and bandwidth is actually not constant as α is dependent on the closed-loop gain. Assuming $A_0 \gg 1$ we note that the low frequency gain is $G = -\alpha/\beta = -R_2/R_1$ implying that (8) for the inverting configuration results in

$$2\pi GBW = \frac{1}{1 + 1/|G|}\omega_c A_0. \tag{9}$$

Only for $|G| \gg 1$ does this equation express a constant gain-bandwidth product.

An important property of feedback is that it reduces distortion, sensitivity to component variations, etc., with a factor of $F(s) = 1 + T(s)$. For the configurations based on voltage mode operational amplifiers we find

$$\begin{aligned} F(s) &= 1 + \frac{R_1}{R_1 + R_2} \times \frac{A_0}{1 + s/\omega_c} \\ &\simeq \begin{cases} \frac{A_0/(|G|+1)+s/\omega_c}{1+s/\omega_c} & \text{inverting amplifier} \\ \frac{A_0/G+s/\omega_c}{1+s/\omega_c} & \text{noninverting amplifier.} \end{cases} \end{aligned} \tag{10}$$

Obviously, $F(s)$ is dependent on the gain G and hence the improvements in distortion, sensitivity, etc., are strongly dependent on G (approximately inversely proportional to G).